Journal of Alloys and Compounds 499 (2010) 135–139

Contents lists available at ScienceDirect

Journal of Alloys and Compounds

journal homepage: www.elsevier.com/locate/jallcom

Influence of doping elements (Y and Fe) on crystal structure and electrical resistivity of the RNi_2 (R = Gd, Er) compounds

B. Kotur[a,*], O. Myakush[a], H. Michor[b], E. Bauer[b]

[a] Department of Inorganic Chemistry, Ivan Franko National University of Lviv, Kyryla and Mefodia St. 6, UA-79005 Lviv, Ukraine
[b] Institute of Solid State Physics, Vienna University of Technology, Wiedner Hauptstrasse 8-10, A-1040 Wien, Austria

ARTICLE INFO

Article history:
Received 5 March 2010
Received in revised form 18 March 2010
Accepted 19 March 2010
Available online 27 March 2010

Keywords:
Rare earth alloys and compounds
Crystal structure
Electrical properties

ABSTRACT

The ternary $R_{0.85}Y_{0.15}Ni_2$ and $RNi_{1.85}Fe_{0.15}$ (R = Gd and Er) phases have been investigated to study the influence of doping elements (Y, Fe) on the crystal structure and electric properties of RNi_2 (R = Gd, Er) based compounds. All substituted alloys show metallic-like conductivity and exhibit anomalies, corresponding to the ferromagnetic phase transition temperatures. Both the Curie temperatures and the scattering contribution from magnetic moments in the paramagnetic state for the binary RNi_2 scale well with the deGennes factor; on the contrary, the Fe-substituted systems strongly deviate.

1. Introduction

Early reports on binary RNi_2 (R = rare earth) classified these intermetallic compounds as belonging to the cubic Laves phases exhibiting the $MgCu_2$ type structure [1]. Subsequently, compositional defects combined with superstructure lines in X-ray diffraction profiles were reported and discussed for several $R_{1-x}Ni_2$ ($0 < x < 0.05$) compounds [2,3]. A first detailed analysis of this superstructure using X-ray and neutron powder diffraction was carried out for YNi_2, demonstrating that a single-phase compound can only be obtained by a stoichiometry 0.95:2. These $Y_{0.95}Ni_2$ samples have been characterized in terms of the space group *F*-43*m* with the lattice parameter *a* doubled and with ordered vacancies on the Y sites 4*a* [4]. A systematic investigation of $R_{1-x}Ni_2$ compounds revealed that this superstructure also exists for other R elements; however, the occupancy of the 4*a* sites increases with decreasing atomic radii of the R elements, reaching 1 for $LuNi_2$ [5,6]. The authors of Refs. [5,7] have obtained a 2*a* superstructure for $Y_{0.95}Ni_2D_{2.6}$, $Tb_{0.95}Ni_2H_{2.5}$ and $Er_{0.98}Ni_2H_{2.5}$ hydrides from X-ray and neutron powder diffraction and established that deuterium leads to re-ordering of the R vacancies.

Investigations of the electrical resistivity of YNi_2 [8] and of transport quantities (resistivity, thermal conductivity, thermopower) of the RNi_2 [9] series evidenced distinct anomalies for some of these compounds at high temperatures. Afterwards, Gratz et al. [10] identified these high-temperature transport anomalies with a structural phase transition from the superstructure type (space group *F*-43*m*) at room temperature to the $MgCu_2$ structure type (space group *Fd*-3*m*) at higher temperatures.

Intermetallic compounds of rare earth elements with 3*d*-elements crystallizing as Laves phases exhibit a large variety of interesting physical properties. Some of these compounds absorb large amounts of hydrogen, thereby inducing changes of their physical properties. Doping of binary compounds by a third element strongly modify their physical and hydrogenation properties, too. Besides, RCo_2 as well as RNi_2 compounds have recently been proposed as materials for magnetocaloric applications because of a large change of entropy revealed at the magnetic phase transition temperature [11]. The maximum entropy gain associated with this phase transition depends on the total angular momentum *J* of the specific rare earth ion, which, however, can be modified by crystalline electric field effects, lifting the $(2J+1)$-fold magnetic moment degeneracy of the rare earth ion. Our previous work [12–17] was focused on the influence of substituting Ni by Fe as well as Er and Gd by Y with respect to the crystal structure, magnetic properties, hydrogenation ability and kinetics of the hydrogenation–dehydrogenation process of alloys based on binary RNi_2 (R = Gd, Er) compounds. All these compounds are very susceptible in absorbing a significant quantity of hydrogen (up to 3.3–3.8 at.H/f.u. at 0.1–0.12 MPa pressure) without a coinciding amorphization. The results of investigations regarding the crystal structure and magnetic properties of $R_{0.85}Y_{0.15}Ni_2$, $RNi_{1.85}Fe_{0.15}$ (R = Gd and Er) and their hydrides were presented in Ref. [17]. For RNi_2 based alloys the substitution of magnetic Gd and Er by non-

* Corresponding author. Tel.: +380 322 727040; fax: +380 322 616903.
E-mail address: kotur@franko.lviv.ua (B. Kotur).

0925-8388/$ – see front matter © 2010 Elsevier B.V. All rights reserved.
doi:10.1016/j.jallcom.2010.03.187

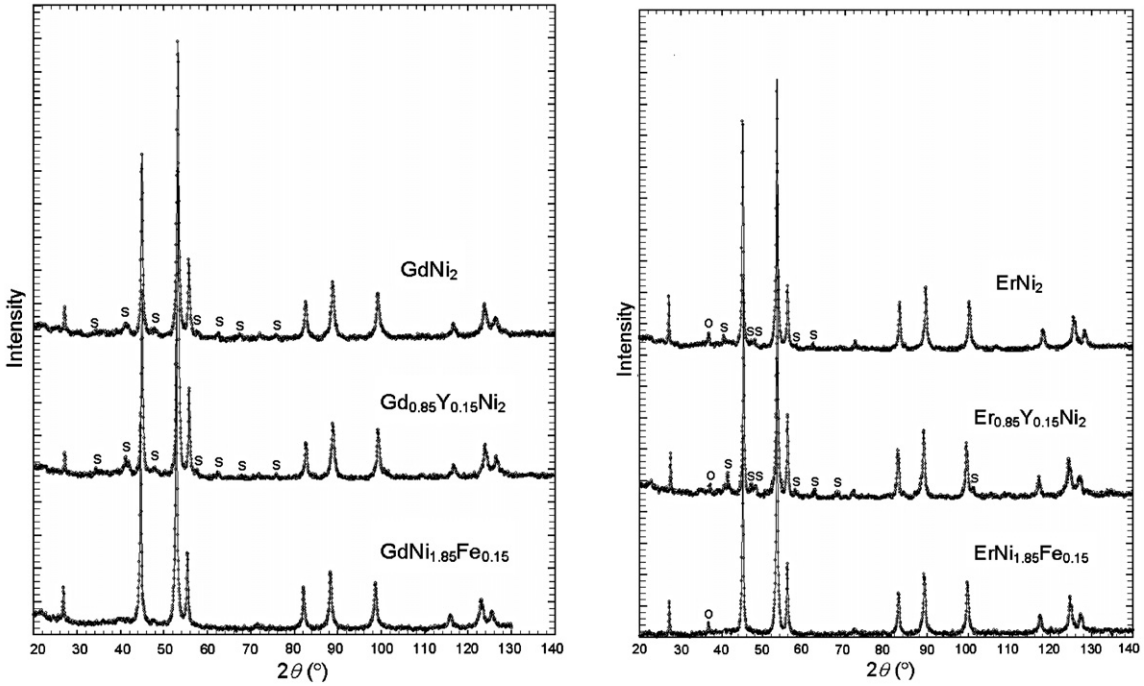

Fig. 1. X-ray powder diffraction patterns of RNi_2 (R = Gd, Er) and doped $R_{0.85}Y_{0.15}Ni_2$, $RNi_{1.85}Fe_{0.15}$ alloys (s-superstructure lines, o-lines of Er_2O_3 oxide).

magnetic Y has minor influence upon T_C; but the Ni/Fe substitution increases T_C from 81 to 217 K for $GdNi_{1.85}Fe_{0.15}$ and from 16 to 118 K for $ErNi_{1.85}Fe_{0.15}$. Hydrogen absorption reduces the saturation moment and suppresses long range magnetic order for the majority of alloys investigated to temperatures below 2 K.

Magnetic properties of the RNi_2 Laves phases with partial substitutions at the R and the Ni sublattices by a third component (R by R', Ni by Co or Fe) as well as of their hydrides have been extensively studied in particular with respect to the interplay between the localized magnetic moments of the rare earth ions and the itinerant electron magnetism of the 3*d* sublattice in these solids leading to a wide variety of magnetic structures and associated magnetic properties [18–20]. Transport properties of these solids, however, are much less investigated. Hence, this report focuses on the influence of Y and Fe substitutions on the crystal structure and electrical resistivity of RNi_2 (R = Gd, Er) compounds.

2. Experimental details

Alloys were prepared by arc melting of the starting elements with a purity not less than 99.9 wt.% under argon. During arc melting the weight losses were less than 1% of the total mass of the ingots. The alloys were annealed in quartz ampoules under vacuum and were homogenated at 600 °C for 720 h.

The samples were examined by X-ray powder diffraction (XRD) using diffractometers HZG-4a (FeKα-radiation) and DRON-3 M (CuKα-radiation). For crystal structure determination the diffraction data were collected using a $\theta - 2\theta$ scan mode with steps of 0.05° and exposition time 20 s at every point. All the crystal structure calculations were performed by the Rietveld method using the programs FullProf [21] and CSD [22].

The temperature dependence of the electrical resistivity was studied by a four probe a.c. method in the temperature range 4–300 K.

3. Results and discussion

XRD patterns of parent RNi_2 (R = Gd, Er) and doped $R_{0.85}Y_{0.15}Ni_2$, $RNi_{1.85}Fe_{0.15}$ alloys are presented in Fig. 1. Detailed analyses of the crystal structures of these compounds are presented in Refs. [13–15]. These patterns of RNi_2 and $R_{0.85}Y_{0.15}Ni_2$ with R = Gd and Er (Fig. 1) were indexed in terms of a cubic symmetry with doubled cell parameter 2*a* (where *a* is the unit cell parameter of the $MgCu_2$ type structure). The existence of superstructure peaks (see Fig. 1) indicates that all samples belong to the $TmNi_2$ structure type. The Fe-containing alloys $GdNi_{1.85}Fe_{0.15}$ and $ErNi_{1.85}Fe_{0.15}$ crystallize in the $MgCu_2$ type structure. There are no visible superstructure lines derived from their XRD patterns (Fig. 1). A small fraction of Er_2O_3 is also present in the Er containing samples (Fig. 1). Refined lattice parameters of the alloys investigated are summarized in Table 1. The final atomic parameters of $Er_{0.85}Y_{0.15}Ni_2$ ($TmNi_2$ structure type) and $ErNi_{1.85}Fe_{0.15}$ ($MgCu_2$ type structure) are presented in Tables 2 and 3.

Figs. 2 and 3 display the temperature dependent electrical resistivity, ρ, of RNi_2 (R = Y, Gd and Er) and $R_{0.85}Y_{0.15}Ni_2$,

Table 1
Crystallographic parameters and Curie temperatures obtained from magnetisation and susceptibility measurements ($^*T_C$) and from resistivity ($^{**}T_C$) of the RNi_2, $R_{0.85}Y_{0.15}Ni_2$ and $RNi_{1.85}Fe_{0.15}$ (R = Gd and Er) alloys.

Compounds	Structure type	Space group	*a* (nm)	$^*T_C$ (K)	$^{**}T_C$ (K)
$GdNi_2$	$TmNi_2$	*F*-43*m*	1.44085(8)	75	73
$ErNi_2$	$TmNi_2$	*F*-43*m*	1.42678(6)	14–16	14
$Gd_{0.85}Y_{0.15}Ni_2$	$TmNi_2$	*F*-43*m*	1.44017(7)	60	62
$Er_{0.85}Y_{0.15}Ni_2$	$TmNi_2$	*F*-43*m*	1.42920(6)	15	13
$GdNi_{1.85}Fe_{0.15}$	$MgCu_2$	*Fd*-3*m*	0.72246(3)	217	215
$ErNi_{1.85}Fe_{0.15}$	$MgCu_2$	*Fd*-3*m*	0.71707(3)	118	118

Table 2
Atomic coordinates and isotropic displacement parameters of $Er_{0.85}Y_{0.15}Ni_2$ ($TmNi_2$ structure type, R_B = 5.05%, R_P = 4.86%, R_{WP} = 10.9%).

Atom	Site	*x*/*a*	*y*/*b*	*z*/*c*	Occupations	$B_{iso} \times 10^2$ (nm^2)
R1	4*a*	0	0	0	0.68(3) Y	1.11(7)
R2	4*b*	1/2	1/2	1/2	1.0 Er	0.72(2)
R3	16*e*	0.6276(2)	*x*	*x*	1.0 Er	0.79(1)
R4	16*e*	0.0975(2)	*x*	*x*	0.52(3)Y + 0.48(3)Er	1.05(1)
R5	24*g*	0.0262(2)	1/4	1/4	1.0 Er	1.02(4)
Ni1	16*e*	0.3046(5)	*x*	*x*	1.0	1.44(2)
Ni2	16*e*	0.8111(6)	*x*	*x*	1.0	1.72(2)
Ni3	24*h*	0.0598(5)	*x*	0.8092(6)	1.0	1.23(2)
Ni4	24*h*	0.0614(5)	*x*	0.3163(7)	1.0	1.64(5)

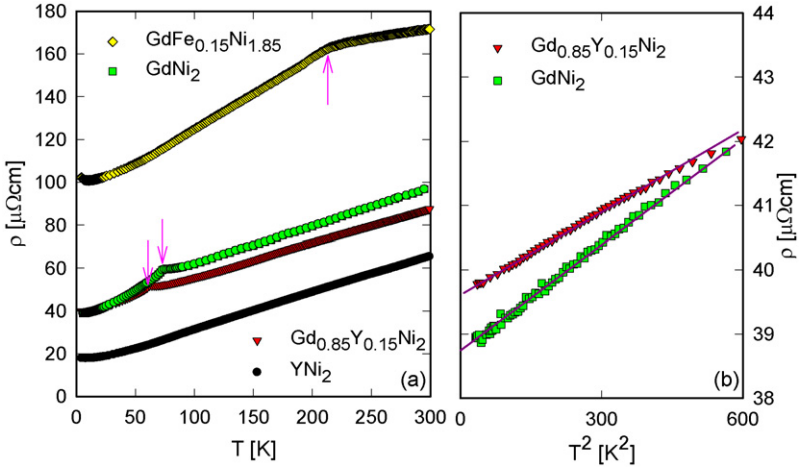

Fig. 2. (a) Temperature dependent electrical resistivity, ρ, of YNi_2, $GdNi_2$, $Gd_{0.85}Y_{0.15}Ni_2$ and $GdFe_{0.15}Ni_{1.85}$. The arrows mark the magnetic phase transition. (b) Temperature dependent electrical resistivity, ρ, of $GdNi_2$ and $Gd_{0.85}Y_{0.15}Ni_2$ plotted on a quadratic temperature scale. The solid lines emphasize the T^2 behaviour of $\rho(T)$.

Table 3
Atomic coordinates and isotropic displacement parameters of $ErNi_{1.85}Fe_{0.15}$ ($MgCu_2$ structure type, $R_B = 4.64\%$, $R_P = 5.17\%$, $R_{WP} = 10.3\%$).

Atom	Site	x/a	y/b	z/c	Occupations	$B_{iso} \times 10^2$ (nm^2)
Er	8*b*	3/8	3/8	3/8	1	1.27(2)
M	16*c*	0	0	0	0.93(1)Ni + 0.07(1)Fe	1.86(4)

$RNi_{1.85}Fe_{0.15}$ (R = Gd and Er) for temperatures from 4 to 300 K. All compounds investigated reveal a metallic-like conductivity. The simplest behaviour is observed for YNi_2, which does neither exhibit magnetic order nor superconductivity. Here, $\rho(T)$ can be accounted for by the Bloch–Grüneisen (BG) formula, where charge carriers (electrons) are treated in terms of the free electron model while phonons are described using the Debye model. Adjusting the BG formula to the experimental data of YNi_2 (solid line, Fig. 3), allows to deduce a temperature independent electron–phonon interaction strength and the Debye temperature $\theta_D = 195$ K. All the remaining alloys shown in Figs. 2 and 3 exhibit long range magnetic order, provoked either by localized magnetic moments (Gd, Er), by the Fe-3*d* moments or by a combination of both. Both, the substituted alloys

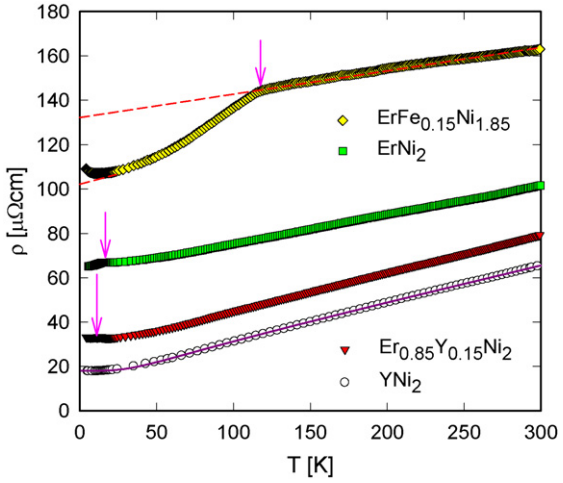

Fig. 3. Temperature dependent electrical resistivity, ρ, of YNi_2, $ErNi_2$, $Er_{0.85}Y_{0.15}Ni_2$ and $ErFe_{0.15}Ni_{1.85}$. The arrows mark the magnetic phase transition. The solid line is a least squares of the Bloch–Grüneisen formula to the experimental data revealing a Debye temperature $\theta_D = 195$ K for YNi_2. The dashed lines sketch the procedure to evaluate ρ_{spd}.

$R_{0.85}Y_{0.15}Ni_2$, $RNi_{1.85}Fe_{0.15}$ (R = Gd and Er), alike the binary analogues $GdNi_2$ and $ErNi_2$ [23,24], are controlled by ferromagnetism [17]. The transition into a ferromagnetically ordered ground state is also apparent from the resistivity data. Increasing order of the magnetic structure on decreasing temperature, i.e., the localized magnetic moments start to arrange right at the ordering temperature and are completely aligned at $T = 0$, is concomitant with a decrease of the electrical resistivity. Also visible from the experimental data is a slight decrease of $\rho(T)$ within a narrow temperature range above T_C. Thus, T_C is rendered by a weak local maximum in the $\rho(T)$ data. The increase of $\rho(T)$ beyond T_C upon lowering the temperature can be understood from ferromagnetic spin fluctuations which develop well above the Curie temperature and which diverge temporally and spatially at T_C. Ferromagnetic order of the materials investigated can be seen from the T^2 dependence of $\rho(T)$ for $T \ll T_C$ (compare Fig. 2(b)). Such a power law is a result of scattering processes of conduction electrons on ferromagnetic spin waves [25]. Interestingly, the Fe-containing materials exhibit at lowest temperatures a minimum in $\rho(T)$ followed by an increase of the resistivity if the temperature is further lowered. A closer inspection of the data reveals nearly logarithmic temperature dependences, which might be a result of Kondo type scattering processes on tiny amounts (~ppm) of Fe which is not fully integrated in the crystalline unit cells. This behaviour is more pronounced in the Er case than in the Gd analogue. For the paramagnetic temperature range (well above T_C), $\rho(T)$ increases almost linearly as a result of the electron–phonon interaction and of the scattering of conduction electrons on the nearly localized disordered magnetic moments (see below). Note also that the absolute change of resistivity is much more pronounced in the cases of $RNi_{1.85}Fe_{0.15}$ than for $R_{0.85}Y_{0.15}Ni_2$. This emphasizes the fact that scattering of conductions electrons on the disordered ligands (Fe–Ni) around the magnetic R ions is much stronger than scattering on disordered Gd–Y. Although there are differences in the scattering cross-section due to the magnetic to non-magnetic state of Gd and Y, the electron configuration [Xe]$4f^7 5d^1 6s^2$ (Gd) and [Kr]$4d^1 5s^2$ (Y) appear not to differ that much; hence scattering is less altered in both cases.

Obviously, the substitution of {Gd, Er} by Y reduces the transition temperatures in both cases (compare Table 1), while the substitution of Ni by Fe yields a substantial increase of the Curie temperature. The former corresponds to a dilution of magnetic Gd or Er by non-magnetic Y; besides the decrease of T_C, the spontaneous magnetisation decreases as well [17]. The 3*d* metal substitution of Ni by 5 at.% Fe sharply increases T_C by a factor of 3–8 for Gd and Er, respectively. This hints at a different mechanism

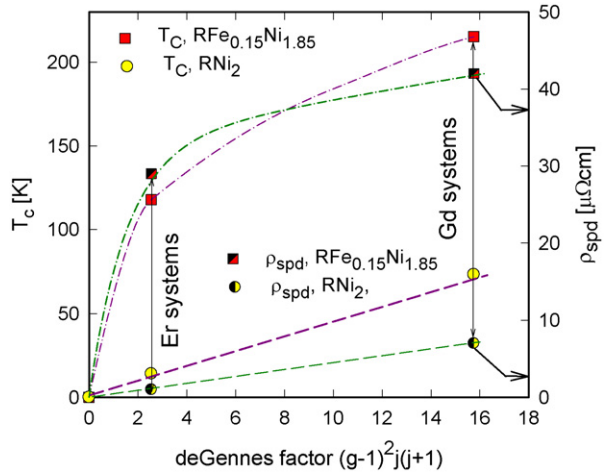

Fig. 4. deGennes scaling of the ferromagnetic phase transition temperature T_C and of the magnetic contribution to the electrical resistivity, ρ_{spd}, for RNi_2 (R = Gd, Er) and $RFe_{0.15}Ni_{1.85}$ (R = Gd, Er). The lines are guides to the eyes.

of ordering compared to the simple RKKY type dominating $GdNi_2$ and $ErNi_2$. Considering RKKY interaction being responsible for the occurrence of long range magnetic order, the so-called deGennes parameter, dG ($T_C \sim dG = (g-1)^2 J(J+1)$, where g is the Lande factor and J the total angular momentum), provides a powerful tool to test such a scenario. Note that the magnetic contribution to the electrical resistivity in the paramagnetic temperature range, ρ_{spd}, scales with the deGennes factor as well. The extrapolation procedure used to determine ρ_{spd} from the experimental $\rho(T)$ data is discussed in detail in Ref. [26]. Crystalline electric field (CEF) effects cause a lifting of the ground state degeneracy, and the thermal population of the various CEF levels provides additional scattering channels. Thus, the spin-disorder resistivity rises with rising temperature. For temperatures above the uppermost CEF level, however, ρ_{spd} remains constant. While for both non-Kramers ions (e.g., Pr or Tb, J is integer) and Kramers ions (e.g. Ce, or Er, J is half-integer) CEF effects create a distinct variety of multiplets located at characteristic energies, the absence of an orbital contribution to J in the case of Gd preserves the degenerate ground state. As a consequence, ρ_{spd} remains constant, too. This can be read off from the linear temperature dependence of ρ_{spd} of $GdNi_2$ well above the ordering temperature. On the other hand, the overall crystal field splitting of $ErNi_2$ is rather small, of the order of 100 K [27], allowing an extrapolation of ρ_{spd} from temperatures above 100 K towards zero. Shown in Fig. 4 is a plot of both T_C and ρ_{spd} as a function of $(g-1)^2 J(J+1)$ for RNi_2 and $RFe_{0.15}Ni_{1.85}$ (R = Gd, Er). Obviously, T_C and ρ_{spd} of $ErNi_2$ and $GdNi_2$ scale well with the deGennes factor, in agreement with other rare earth intermetallics such as RAl_2 [26] or RPt [28]. This, however, is not the case for $RFe_{0.15}Ni_{1.85}$. Both, T_C and ρ_{spd} are far-off from scaling; rather, both quantities seem to be underpinned by some constant background, upon which there is a contribution, roughly proportional to the deGennes parameter. From a more microscopic point of view, the non-negligible magnetic moment of Fe (1.45 μ_B/Fe in YFe_2 or 1.6 μ_B/Fe in $GdFe_2$ [29]), as well as the high ordering temperatures in binary RFe_2 (545 K for YFe_2 and 785 K for $GdFe_2$ [29]) substantially influence electronic transport in the intermetallics described above and, specifically, T_C and ρ_{spd} of $RFe_{0.15}Ni_{1.85}$ (R = Gd, Er). Since the shape of the $\rho(T)$ curves in the paramagnetic temperature range does not change substantially upon the Fe substitution, one might conclude that scattering of the conduction electrons on the Fe moments is qualitatively similar to that on the localized rare earth moments, although there is a distinct quantitative difference. Consequently, the Fe-3*d* moments should behave localized rather than itinerantly. In fact, band structure calculations carried out for YFe_2 and $LuFe_2$ [30] clearly evidence the localized character of the Fe-3*d* states from narrow features in the electronic density of states above and below the Fermi energy E_F.

4. Conclusion

RNi_2 (R = Gd, Er) and doped $R_{0.85}Y_{0.15}Ni_2$, $RNi_{1.85}Fe_{0.15}$ alloys have been studied by X-ray diffraction and temperature dependent electrical resistivity. While the latter crystallize in the $MgCu_2$ structure, both former groups exhibit a defect structure of the $TmNi_2$-type with ordered vacancies on the rare earth site at room temperature, which, however, become disordered above a structural phase transition at high temperatures [10]. The ground state properties are dominated by ferromagnetism of the rare earth ions Gd and Er. While, upon substitution, non-magnetic Y causes a dilution of magnetic moments on the rare earth site, resulting in a decrease of the ordering temperature, adding Fe instead of Ni improves the magnetic exchange coupling and shifts the phase transition towards higher temperatures. This additional contribution to the magnetic state in the pseudo-binaries leads to substantial deviations from deGennes scaling.

Acknowledgement

This work was supported by the Ukrainian-Austrian WTZ project No. UA 06/2009.

References

[1] R.H. Van Essen, K.H.J. Buschow, J. Less-Common Met. 70 (1980) 189–198.
[2] V. Paul-Boncour, A. Perchéron-Guegan, M. Escorne, A. Mauger, J.C. Achard, Z. Phys. Chem. 163 (1989) 263.
[3] A.F. Deutz, R.B. Helmoldt, A.C. Moleman, D.B. de Mooij, K.H.J. Buschow, J. Less-Common Met. 153 (1989) 259–266.
[4] M. Latroche, V. Paul-Boncour, A. Perchéron-Guegan, J.C. Achard, J. Less-Common Met. 161 (1990) L27–L31.
[5] M. Latroche, V. Paul-Boncour, A. Perchéron-Guegan, Z. Phys. Chem. 179 (1993) 261–268.
[6] V. Paul-Boncour, A. Lindbaum, M. Latroche, S. Heathman, Intermetallics 14 (2006) 483–490.
[7] A. Perchéron-Guegan, V. Paul-Boncour, M. Latroche, J.C. Achard, F. Bouree-Vigneron, J. Less-Common Met. 172–174 (1991) 198–205.
[8] A. Slebarski, J. Less-Common Met. 141 (1988) L1–L7.
[9] J.M. Fournier, E. Gratz, in: K.A. Gschneidner Jr., L. Eyring, G.H. Lander, G.R. Choppin (Eds.), Handbook on the Physics and Chemistry of Rare Earths, vol. 17, North-Holland, Amsterdam, 1993, p. 409.
[10] E. Gratz, A. Kottar, A. Lindbaum, M. Mantler, M. Latroche, V. Paul-Boncour, M. Acet, Cl. Barner, W.B. Holzapfel, V. Pacheco, K. Yvon, J. Phys.: Condens. Matter 8 (1996) 8351–8361.
[11] J. Cwik, T. Palewski, K. Nenkov, J. Ljubina, J. Klamut, J. Low Temp. Phys. 159 (2010) 37–41.
[12] O. Myakush, Yu. Verbovytsky, B. Kotur, I. Kovalchuk, V. Beresovetz, I. Zavaliy, J. Phys.: Conf. Ser. 79 (2007) 012018.
[13] O.R. Myakush, Yu.V. Verbovyts'kyi, V.V. Berezovets', O.H. Ershova, V.D. Dobrovol's'kyi, B.Ya. Kotur, Mater. Sci. 43 (2007) 682–688.
[14] O.R. Myakush, Yu.V. Verbovytsky, I.V. Koval'chuck, R.V. Denys, V.V. Berezovets, B.Ya. Kotur, X. Internat, Conf. on Crystal Chemistry of Intermetallic Compounds, Lviv, Ukraine, September 17–20, 2007, p. 73.
[15] B. Kotur, Yu. Verbovytsky, O. Myakush, I. Kovalchuk, V. Berezovets, Internat. Conf. on Solid Compounds of Transition Elements, Dresden, July 26–31, 2008.
[16] B. Kotur, O. Myakush, I. Zavaliy, Croat. Chem. Acta 82 (2009) 469–476.
[17] H. Michor, B. Kotur, O. Myakush, G. Hilscher, J. Phys.: Conf. Ser. (submitted for publication).
[18] K.H.J. Buschow, in: K.A. Gschneidner Jr., L. Eyring (Eds.), Handbook on the Physics and Chemistry of Rare Earths, vol. 10, North-Holland Publishing Co., 1984, pp. 1–111.
[19] K. Yvon, P. Fischer, Crystal and Magnetic Structures of Ternary Metal Hydrides: A Comprehensive Review, in: Topics in Applied Physics, Vol. 63, Hydrogen in Intermetallic Compounds I. Electronic, Thermodynamic and Crystallographic Properties, Preparation, Springer-Verlag, Berlin, 1988, pp. 87–138.
[20] G. Wiesinger, G. Hilscher, in: K.H.J. Buschow (Ed.), Handbook on Magnetic Materials, vol. 17, Elsevier B.V, 2008, pp. 293–456 (Chapter 5).
[21] J. Rodrigues-Carvajal, Program: FullProf. Lab. Leon Brillouin, CEA-CNRS, 1998.
[22] L.G. Akselrud, P.Yu. Zavalii, Yu.N. Grin, V.K. Pecharsky, B. Baumgartner, E. Wolfel, Mater. Sci. Forum 133–136 (1993) 335–340.

[23] S.K. Malik, W.E. Wallace, Solid State Commun. 24 (1977) 283–285.
[24] E. Burzo, A. Chełkowski, H.R. Kirchmayr, in: H.P.J. Wijn (Ed.), Landolt-Börstein, Numerical Data and Functional Relationship in Science and Technology, New Series, Magnetic Properties of Metal, vol. 19-D2, Springer, Berlin, 1990.
[25] G.T. Meaden, Contemp. Phys. 12 (1971) 313.
[26] E. Gratz, M.J. Zuckermann, in: K.A. Gschneidner Jr., L. Eyring (Eds.), Handbook on the Physics and Chemistry of Rare Earths, North-Holland Publishing Co., 1982 (Chapter 42).
[27] J.J. Melero, R. Burriel, M.R. Ibarra, J. Magn. Magn. Mater. 140–144 (1995) 841–842.
[28] E. Gratz, E. Bauer, H. Nowotny, J. Magn. Magn. Mater. 70 (1987) 118–125.
[29] H. Kirchmayr, C.A. Poldy, in: K.A. Gschneidner Jr., L. Eyring (Eds.), Handbook on the Physics and Chemistry of Rare Earths, North-Holland Publishing Co., 1979 (Chapter 14).
[30] E. Gratz, E. Bauer, H. Nowotny, A.T. Burkov, M.V. Vedernikov, Solid State Commun. 69 (1989) 1007–1010.